Asian Journal of Chemistry; Vol. 36, No. 7 (2024), 1592-1600

ASIAN JOURNAL OF CHEMISTRY

https://doi.org/10.14233/ajchem.2024.31673

Spectrophotometric Study of the Effect of Micellar Medium on the Dissociation Equilibrium of Sulfonephthalein pH Indicator Dye

SUBHODIP SAMANTA

Department of Chemistry, Maulana Azad College, Kolkata-700013, India

Corresponding author: E-mail: subhodip.samanta@gmail.com

Received: 6 April 2024; *Accepted*: 16 May 2024; *Published online*: 29 June 2024; AJC-21679

The experimental determination of the mono-dianionic dissociation equilibrium constant ($pK_{a_2}^{m}$) of sulfonephthalein pH-indicator dye bromocresol green (BCG) in cetyltrimethylammonium bromide (CTAB) micellar media revealed a deviation from its value in pure water ($pK_{a_2}^{w}$). This discrepancy indicates that the presence of CTAB micellar media alters the dissociation behaviour of BCG compared to its behaviour in pure water. Such alterations suggest that the micellar environment influences the protonation and deprotonation processes of the dye molecule, likely through interactions between the dye and the micellar environment. To further understand this phenomenon, theoretical models depicting the dissociation equilibrium of BCG in aqueous micellar solutions were employed. These models utilized non-linear regression analysis methods integrated into microsoft excel solver. The calculations involved the use of spectrophotometrically determined binding constants (k_b) and partition coefficients (K_x) of the dye between the micellar pseudo phase and water. The obtained $pK_{a_2}^{m}$ values for BCG in different pH media were found to be varied. This variability was attributed to the flexible extent of solubilization of the dianionic form of BCG in the CTAB micellar medium, which changes with variations in aqueous pH. The observed relative intensity of absorption bands of mono and dianionic forms of the dye in the micellar medium correlated with these differences in $pK_{a_2}^{m}$ magnitudes.

Keywords: Bromocresol green, Indicator dissociation constant, Micelles, UV-Vis spectra, Binding constant, Partition coefficient.

INTRODUCTION

Sulfonephthalein dyes have found widespread application in various scientific and industrial domains, serving as valuable probes for investigating changes in the physico-chemical characteristics of aqueous environments. Significantly, they play a crucial role in determining the surface pH of micelles, elucidating dye-surfactant interactions and facilitating analytical and industrial chemistry processes [1-4]. Researchers have dedicated significant efforts to unraveling the intricacies of the acid-base equilibria exhibited by these dyes. A key strategy involves discerning the influences governing these equilibria by comparing the equilibrium constants in water ($K_{a_2}^{w}$) with the apparent acid-base equilibrium constant ($K_{a_2}^{m}$) observed exclusively within the interfacial microenvironment of the micelles. This comparative analysis helps in identifying the distinct factors contributing to the overall acid-base behaviour of the sulfonephthalein dyes, thus enhancing our understanding of their behaviour in diverse contexts [5-12]. The shifts observed in the $pK_{a_2}^{m}$ values of aqueous indicator dyes in the presence of surfactants can be attributed to various factors. These include the electrostatic potential existing at the surface of micelles, ion exchange processes occurring between the micelle surface and the bulk aqueous phase, formation of ion pairs between oppositely charged indicator species and head groups of monomeric surfactants, low interfacial effective relative permittivity, interfacial salt effects and other specific molecular interactions [5-9]. Most of the studies conducted thus far have focused on systems where the dye is either completely micellized or binds to the micelles in both its acidic and basic forms. Also, there have been studies examining the acid-base equilibria of indicator dyes in aqueous ionic micellar media, where the dye is only partially bound to the micelles [5-9]. Still, there is a clear shortage of studies on the acid-base equilibria employing indicator dyes not entirely absorbed into micelles.

In this study, the partitioning behaviour of the sulfonephthalein pH indicator dye bromocresol green (BCG) between cetyltrimethylammonium bromide (CTAB) micellar pseudo-

phase and water phase across three different aqueous pH buffer medium (pH 3.8, 5.3 and 7.0) using spectrophotometric methods were investigated. The UV-Vis absorption spectra of BCG were analyzed, with a focus on the variation in CTAB concentration under fixed pH conditions. By analyzing these spectra, the binding constants (k_b) and the free energy of binding (ΔG_b°) for the BCG-CTAB association, employing the Benesi-Hildebrand equation were determined with varying pH of the media. Additionally, the partition coefficient values (K_c) characterizing the partitioning of BCG molecules between the pseudo micellar phase and water, along with the fraction of BCG molecules retained by the CTAB micelle, were calculated. The theoretical models were employed in this study to depict the dissociation equilibrium of bromocresol green in aqueous micellar solutions. These models were then utilized to calculate the theoretical $pK_{a_2^m}^m$ values using non-linear regression analysis methods integrated into microsoft excel solver. The calculations relied on the experimentally determined binding constants and partition coefficients of the dye between the micellar pseudo phase and water. By utilizing these theoretical models and incorporating experimental data, the $pK_{a_2^m}^m$ values of bromocresol green in the CTAB micellar environment were determined. This approach allowed for a quantitative assessment of the dissociation equilibrium of the dye within micellar solutions, providing valuable insights into its behaviour under different experimental conditions. This comprehensive approach sheds light on the behaviour of BCG within the CTAB-micellar environment under different experimental conditions, contributing to understanding of its solubilization and interaction dynamics.

EXPERIMENTAL

Cetyltrimethylammonium bromide (CTAB), molar mass 364.45 g/mol, AR, Merck and bromocresol green (BCG) sodium salt, molar mass 720.02 g/mol, AR, Merck were used. All solutions were meticulously prepared using deionized water, ensuring a conductivity of less than 3.00×10^{-6} S to maintain the purity of the solutions. Buffers of pH 3.8, pH 5.3 and pH 7.0 were meticulously prepared by appropriately mixing acetic acid and sodium hydroxide to achieve the desired pH levels. To prepare the experimental solutions, initial stock solutions of CTAB (10^{-2} M) and BCG (10^{-3} M) in water at pH 3.8, pH 5.3 and pH 7.0, respectively were prepared. From these stock solutions, by proper mixing, the chosen range of solutions of CTAB (0.05 mM to 4 mM) in the fixed concentration of BCG (10^{-4} M) were prepared.

A digital conductivity meter, specifically the Systronics-304 model, was employed to measure the conductivity of the studied systems. This instrument offers a resolution level of ± 0.1 µS, ensuring precise measurements. Prior to each use, the conductivity meter underwent calibration using standard 0.1 M and 0.01 M KCl solutions to ensure accuracy and reliability of the measurements. UV-vis absorption measurements were conducted using a Perkin-Elmer spectrophotometer, with the Lambda 55 model being employed in this experiment. All data analysis, including the generation of graphs and calculations, was carried out using MS Excel software.

The CMC values of CTAB in the presence of 10^{-4} M BCG at the experimental condition of varying aqueous pH of 3.8, 5.3 and 7.0, respectively were determined from the plots of specific conductance *versus* the concentration of surfactants [13,14]. The CMC values of CTAB in the presence of BCG exhibited a slight decrease with increasing pH of the medium. At pH 3.8, the CMC was 0.87 mM, while at pH 5.3 and pH 7.0, the CMC values were 0.85 mM and 0.81 mM, respectively.

RESULTS AND DISCUSSION

Absorption spectra of bromocresol green (BCG) in aqueous solutions: The absorption spectra of bromocresol green (BCG) in aqueous solutions provide valuable insights into its molecular behaviour under varying pH conditions (Fig. 1, inset). In aqueous media, BCG exists in an equilibrium between its monoanionic and dianionic forms. This equilibrium is pH-dependent, with the relative composition of the two forms determined by the acidity or basicity of the solution. The reported pK_a value of BCG, indicating the pH at which the concentration of the two forms is equal, is 4.7 [15,16]. Below this pH, the monoanionic form predominates, while above it, the dianionic form becomes more prevalent. At pH 3.8, corresponding to acidic conditions, BCG primarily takes the monoanionic form. This was reflected in the absorption spectrum by the presence of band-2, observed in the wavelength range of 350-450 nm. Conversely, at pH 7.0, BCG predominantly exists in the dianionic form. This results in the appearance of band-3, observed in the wavelength range of 450-700 nm (Fig. 1, inset). The absorption peak (λ_{max}) at approximately 616 nm in neutral pH solutions corresponds to the absorption of the dianionic form of BCG, contributing to the blue colour observed in such solutions. The distinct absorption bands observed in the absorption spectra of BCG at different pH levels provide a direct means of characterizing its molecular state in solution.

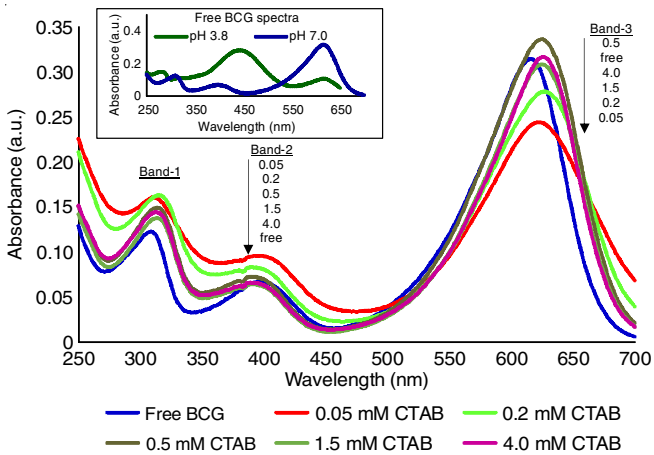

Fig. 1. Absorption spectra of 0.1 mM of BCG in aqueous CTAB (range-0.05 mM to 4 mM) at pH 7.0 and at 303 K (Inset: spectra of aqueous solution of free BCG in acidic and neutral pH)

Absorption spectra of aqueous solution of BCG in the presence of CTAB at pH 7.0: The absorption spectra of BCG-CTAB solutions provide valuable insights into the interactions between BCG and CTAB surfactant under aqueous conditions

at pH 7.0 (Fig. 1). The intensity of the absorbance band (Band-3) corresponding to the dianionic form of BCG varies with the gradual increase in CTAB concentration while maintaining a fixed BCG concentration. In the pre-micellar region of CTAB (0.05 mM), an initial decrease in the intensity of band-3 was observed. However, as CTAB concentration increases, the intensity of band-3 gradually increases. In the post-micellar region (3-4 mM CTAB), the intensity of band-3 saturates, indicating maximum solubilization of BCG in the micellar core. The initial decrease in band-3 intensity suggests the ion-pair formation between the anionic BCG and cationic CTAB, reducing the concentration of free dye molecules in solution [17-29]. Subsequent increase in band-3 intensity with increasing CTAB concentration indicates the penetration of BCG molecules into the micellar surface, facilitating effective orientation for light absorption [27,28]. Also, the absorption maxima of band-3 (dianionic form) shift slightly towards longer wavelengths (bathochromic shift) from 616 to 626 nm with increasing CTAB concentration. Conversely, a small shift in the absorption maxima of band-2 (monoanionic form) towards shorter wavelengths (hypsochromic shift) was observed from 400 nm to 410 nm. The observed shifts in absorption maxima suggest gradual solubilization of hydrophobic BCG in the CTAB micellar surface with increasing CTAB concentration [28]. Electrostatic attraction between the negatively charged sulphonate group of BCG and the positive head groups of CTAB micelles allows penetration of BCG molecules only into the outer region of the micellar surface (Stern layer) [29-36].

Absorption spectra of BCG-CTAB system at aqueous pH 3.8 and 5.3: The absorption spectra (Fig. 2) depict the changes in the BCG-CTAB system under fixed aqueous pH conditions. At pH of 3.8, the intensity of absorption band-3, corresponding to the dianionic form of BCG, increases gradually upon the addition of CTAB solutions to the BCG solution . Additionally, the absorption peak (λ_{max}) shifts from 619 nm in pure aqueous medium to 627 nm in the presence of CTAB. This shift suggests a perturbation of the monoanionic-dianionic equilibrium of the BCG moiety in the aqueous medium induced by the addition of CTAB solutions. The observed increase in the intensity of band-3 and the shift in λ_{max} upon the addition of CTAB to the BCG solution indicate alterations in the equilibrium between the monoanionic and dianionic forms of BCG.

Effect of CTAB addition on acid-base equilibria of BCG forms: To investigate the impact of CTAB addition on the acid-base equilibria of the monoanionic and dianionic forms of bromocresol green (BCG) in aqueous medium, the ratio of the intensity maxima of band-3 to that of band-2 ($I_{max}^{band\text{-}3} / I_{max}^{band\text{-}2}$) was calculated at different pH levels (3.8, 5.3, 7.0). These ratios were then plotted against the concentration of CTAB solution added (Fig. 3).

At pH 3.8 and 5.3, the $I_{max}^{band\text{-}3} / I_{max}^{band\text{-}2}$ ratio initially increases with the gradual addition of CTAB in the pre-micellar region. This initial increase suggests preferential solubilization or complex formation of the dianionic form of BCG with CTAB micelles. In the CMC region of CTAB, the ratio saturates, indicating complete solubilization of BCG in the CTAB micelles. A slight decrease in the ratio in the post-micellar region

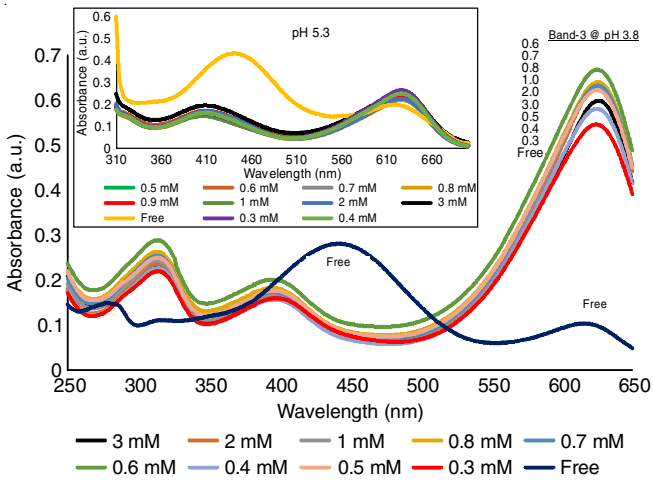

Fig. 2. Absorption spectra of 0.1 mM of BCG in aqueous CTAB solution at pH 3.8 (range-0.3 mM to 3 mM) at 303 K (Inset: absorption spectra of 0.1 mM of BCG in aqueous CTAB solution at pH 5.3 (range-0.3 mM to 3 mM) at 303 K)

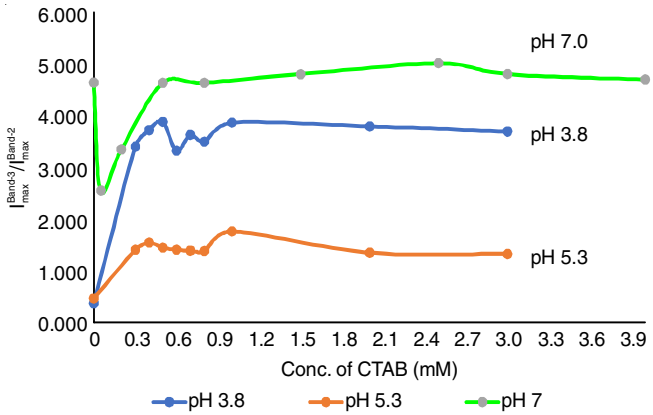

Fig. 3. Ratio of maximum intensity of Band-3 to that of Band-2 in the aqueous pH 3.8, 5.3, 7.0, respectively and in the presence of isopropanol cosolvent at 303 K

suggests variations in the indicator dissociation constant of BCG in CTAB-micellar media compared to that in pure water [5-9]. At pH 7.0, an initial decrease followed by an increase in the ratio was observed in the pre-micellar region of CTAB. Again, a small decrease in the intensity ratio was observed in the post-micellar region. The observed trends in the ratio of $I_{max}^{band\text{-}3} / I_{max}^{band\text{-}2}$ reflect the dynamic interactions between CTAB and BCG molecules in aqueous solution. Changes in the intensity ratio indicate alterations in the equilibrium between the mono-anionic and dianionic forms of BCG and their interactions with CTAB micelles.

Determination of partition coefficient (K_c, dm^3 mol^{-1}): The solubilization of BCG dye in CTAB micelles can be measured using the partition coefficient (K_c) between the CTAB-micellar pseudo phase and water. The partition coefficient was calculated using the equation proposed by Kawamura *et al.* [22,25,37], which is based on the pseudo-phase model approximation:

$$\frac{1}{\Delta A} = \frac{1}{\Delta A_{\infty}} + \frac{1}{K_c \Delta A_{\infty}} \left(\frac{1}{C_d + C_s + CMC_0} \right) \quad (1)$$

where C_d = total BCG concentration, C_s = concentration of the surfactant CTAB, CMC_0 = the CMC of CTAB in water, ΔA ($A-A_0$) is the difference in absorbance value of BCG at any surfactant concentration (A) and to that of the absence of surfactant (A_0). Similarly, ΔA_∞ is the difference in absorbance value at the infinity concentration of surfactant (A_∞) to that of the absence of surfactant (A_0). K_c is the partition coefficient (dm^3 mol^{-1}) of the BCG between the CTAB micellar phase and water. The plots of $1/\Delta A$ *versus* $1/(C_d + C_s - CMC_0)$ were found to be fitted linearly, yielding good correlation coefficient (r^2) values (Fig. 4a). From the slope and the intercept of the linearly fitted curves, the partition coefficient K_c (dm^3 mol^{-1}) values were calculated. The K_x values, corresponding dimensionless partition coefficients, were also determined using the relation $K_x = K_c \times n_w$, where nw is the number of moles of water per dm^3 (55.5 mol dm^{-3}). The standard free energy change (ΔG°_p) associated with the transfer of BCG molecules from bulk water to the CTAB micellar surface was calculated using the relation:

$$\Delta G^\circ_p = -RT \ln K_x$$

where T is the temperature in Kelvin and R is the universal gas constant.

The negative ΔG°_p values demonstrate spontaneous solubilization of BCG in CTAB micelles under all the experimental conditions (Table-1). In water medium, the K_x values decrease with increasing pH, with the highest value observed at pH 3.8 and the lowest at pH 7.0. The observed trends in K_x values suggest variations in solubilization behaviour based on the acidity of medium.

TABLE-1
PARTITION COEFFICIENTS (K_c & K_x) OF BCG-CTAB COMPLEXES AT 303 K

Medium	K_c (dm^3 mol^{-1})	K_x	ΔG°_p (kJ mol^{-1})
Aqueous pH 7.0	1.87×10^3	1.04×10^5	-29.09
Aqueous pH 5.3	2.07×10^3	1.15×10^5	-29.35
Aqueous pH 3.8	2.19×10^3	1.22×10^5	-29.50

Determination of binding constants: The binding constants (k_b) for the association between BCG and micellized CTAB were calculated using the modified Benesi-Hildebrand equation [27,32,38]. The equation relates the total concentration of the dye (C_d) to the difference in absorbance (ΔA), the molar absorptivity of dye (ε_m), the molar absorptivity of fully bound dye to micelle (ε_0), the concentration of micellized surfactant (C_m) and the binding constant (k_b) as follows:

$$\frac{C_d}{\Delta A} = \frac{1}{\varepsilon_m - \varepsilon_0} + \frac{1}{K_b(\varepsilon_m - \varepsilon_0)}\frac{1}{C_m} \quad (2)$$

Plots of $C_d/\Delta A$ against $1/C_m$ were found to be linear in aqueous pH 3.8, 5.3 and 7.0 (Fig. 4b). From the linear regression analysis of the plots, the binding constants (k_b, dm^3 mol^{-1}) values were calculated (Table-2). The standard free energy change of the binding (ΔG°_b) was also calculated from the binding constants applying the relation: $\Delta G^\circ_b = -RT \ln k_b$. The negative ΔG°_b values (Table-2) indicate that the binding of dye to the surfactant is spontaneous under all the experimental conditions.

TABLE-2
BINDING CONSTANTS (K_b) AND pH INDEPENDENT ASSOCIATION CONSTANT (K_s) OF BCG-CTAB COMPLEXES AT 303 K

Medium	K_b (dm^3 mol^{-1})	ΔG°_b (kJ mol^{-1})	K_s (dm^3 mol^{-1})	f_{mic}
pH 7.0	1.25×10^3	-17.96	2.75×10^5	0.757
pH 5.3	1.41×10^3	-18.26	2.56×10^3	0.779
pH 3.8	2.08×10^3	-19.25	2.37×10^3	0.839

The pH-independent binding constant (k_s) was calculated using equation [39]:

$$k_s = k_b\left(1 + \frac{k_{a_2^w}}{[H_w^+]}\right) \quad (3)$$

where $k_{a_2^w}$ = dissociation constant of dye in water (determined experimentally, Table-3) and $[H_w^+]$ = concentration of $[H^+]$ ion in water.

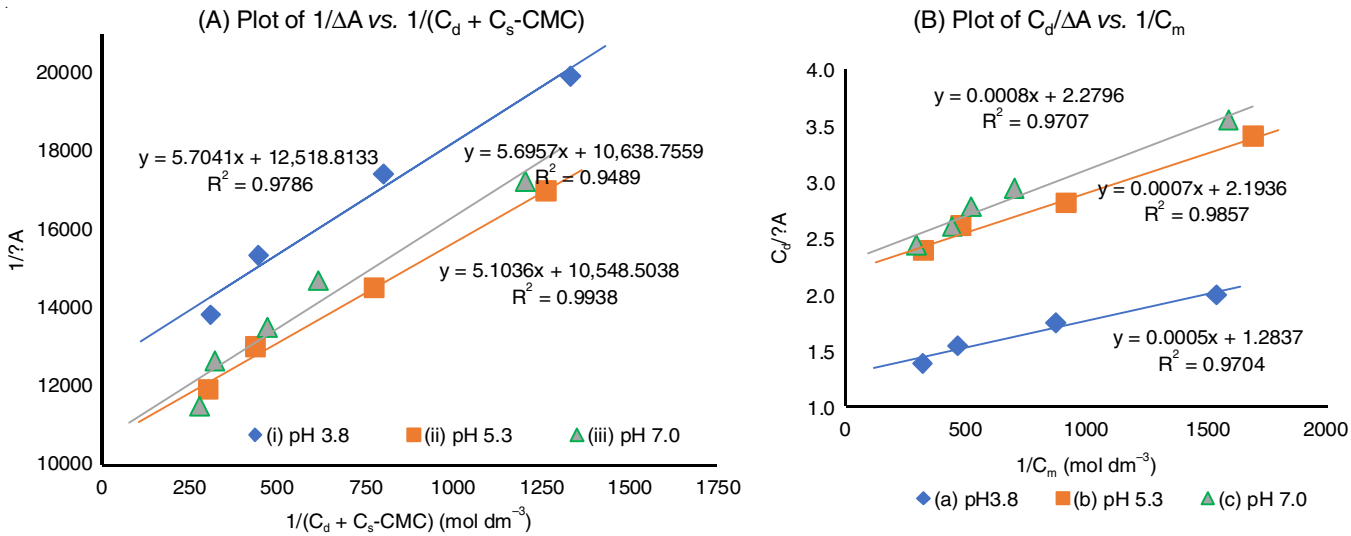

Fig. 4. (A) Determination partition coefficient (K_c): Plots of $1/\Delta A$ *vs.* $1/(C_d + C_s\text{-}CMC_0)$ in (i) pH 3.8 (ii) pH 5.3 (iii) pH 7.0; (B) determination binding constant (k_b): Plots of $C_d/\Delta A$ *vs.* $1/C_m$ in (a) pH 3.8 (b) pH 5.3 (c) pH 7.0

TABLE-3
INDICATOR DISSOCIATION CONSTANTS ($k_{a_2^m}$) OF BCG IN CTAB MICELLAR MEDIA DETERMINED BY METHOD-1

pH	Abs (D_w^{2-})	α	Abs (D_m^{2-})	$k_{a_2^m}$
3.8	0.103	7.62×10^{-5}	0.636	1.49×10^{-4}
5.3	0.212	3.44×10^{-4}	0.267	5.63×10^{-5}
7.0	0.318	3.12×10^{-4}	0.317	9.44×10^{-6}

The magnitude of the binding constant of BCG-CTAB association (k_b) was found to be the highest for aqueous pH 3.8. As the pH of the medium increases, the magnitude of binding constants gradually decreases. The pH independent binding constants (k_s) show a reverse trend compared to the pH dependent binding constants (k_b) (Table-2). This indicates that the pH of the micellar media influences the binding equilibrium of dye with surfactant micelle.

The pH dependent binding constants (k_b) increase with the decrease in the pH of medium. Binding constants ultimately reach a value close to the pH independent binding constant. Overall, the data suggests that pH plays a significant role in the binding equilibrium of BCG with CTAB micelle, with lower pH favouring stronger binding. Fraction of dye incorporated in the micellar surface (f_{mic}) can be calculated following the equation [29,40]:

$$f_{mic} = \frac{k_b M}{1 + k_b M} \quad (4)$$

where, M is any concentration of the surfactant after the CMC of surfactant. The f_{mic} values were calculated under different experimental conditions of the present study taking 'M' as 2.5 mM in all the calculations and the values are shown in Table-2. The results reveal that the retention capacity of CTAB micelle for BCG dye (f_{mic}) decreases as the pH of medium increases.

Dissociation equilibria of BCG in the presence of CTAB: The dissociation equilibrium of BCG dye in aqueous CTAB solution can be theorized as shown in **Scheme-I**. Where, DH_w^- and DH_m^- are the monoanionic forms of BCG, D_w^{2-} and D_m^{2-} are the dianionic forms of BCG and H_w^+ and H_m^+ are the hydrogen ion concentrations in water and in micellar pseudo phase respectively. In the **Scheme-I**, the mono-dianionic dissociation equilibrium constant in water phase is represented by $k_{a_2^w}$ and the dissociation equilibrium constant in CTAB-micellar pseudo phase is denoted by $k_{a_2^m}$. In present work, the $k_{a_2^m}$ was assessed through two distinct theoretical methodologies, which were

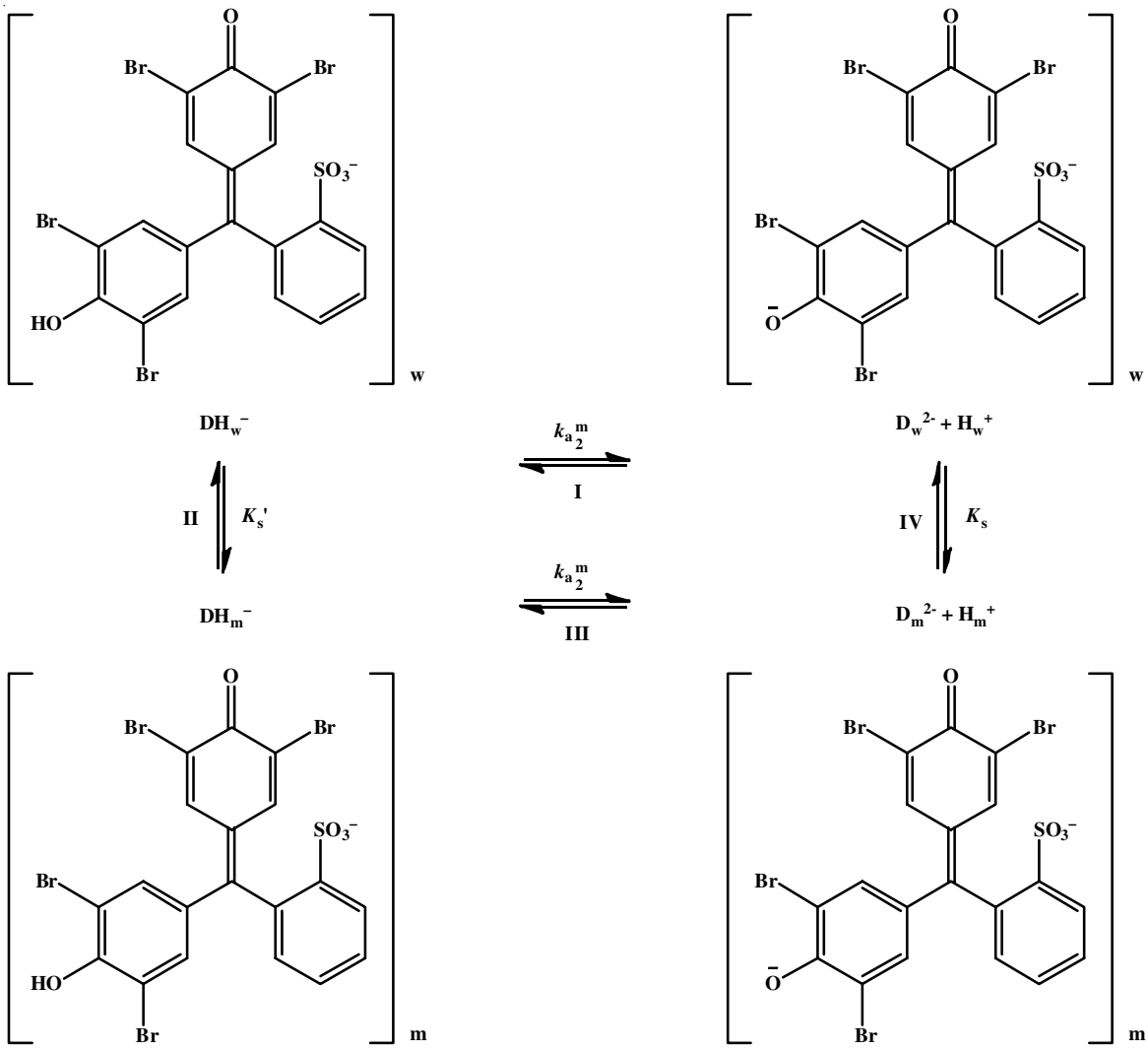

Scheme-I: Dissociation equilibrium of bromocresol green (BCG) in micellar (m) and water (w) media

reported in the literature: Method-1 [9] and Method-2 [7,8,40]. The $k_{a_2^m}$ values calculated by theoretical methods were then compared with the experimentally determined $k_{a_2^m}$ values.

Method-1: Considering the equilibrium-I as represented in **Scheme-I**, the dissociation constant of BCG in water medium ($k_{a_2^w}$) can be written as [9]:

$$k_{a_2^w} = \frac{[H_w^+][D_w^{2-}]}{C_0 - [D_w^{2-}]} \quad (5)$$

where C_0 is the total concentration of dye in the water.

Applying the Beer's law, we get:

$$A(D_w^{2-}) = \varepsilon(D_w^{2-})\, b\, [D_w^{2-}] \quad (6)$$

where $A(D_w^{2-})$ is the absorbance of D_w^{2-} in water and $\varepsilon(D_w^{2-})$ is the molar absorptivity of D_w^{2-}. Assuming $\varepsilon(D_w^{2-})\, b$ = constant = α^{-1}, we get $[D_w^{2-}] = \alpha\, A(D_w^{2-})$.

So, eqn. 5 can be rearranged as:

$$k_{a_2^w} = \frac{[H_w^+]A(D_w^{2-})\alpha}{C_0 - A(D_w^{2-})\alpha} \quad (7)$$

$$\text{or,} \quad \alpha = \frac{k_{a_2^w} C_0}{([H_w^+] + K_{a_2^w})A(D_w^{2-})} \quad (8)$$

Eqn. 8 was used to calculate the α values at three different experimental pHs and are shown in the Table-3. Subsequently, $k_{a_2^m}$ values were calculated following equation (considering equilibrium-III of **Scheme-I**):

$$k_{a_2^m} = \frac{[H_w^+]A(D_m^{2-})\alpha}{C_0 - A(D_m^{2-})\alpha} \quad (9)$$

where it is assumed that the pH of micellar medium remains the same as that of the respective pH of the aqueous medium. The results show that with the increase in pH of medium, the magnitude of apparent dissociation constant of BCG in micellar medium ($k_{a_2^m}$) decreases (Table-3).

Method-2: In the second method to calculate $k_{a_2^m}$, the overall dissociation equilibrium of BCG in the CTAB micellar solution was considered, in view of multiple equilibria (equilibrium-I, II, III and IV, **Scheme-I**) [7,8,40]. The $k_{a_2^m}$ of the BCG at any concentration of CTAB is respresented as:

$$k_{a_2^m} = \frac{([D_w^{2-}] + [D_m^{2-}])[H_w^+]}{([DH_w^-] + [DH_m^-])} \quad (10)$$

To calculate the apparent dissociation constant ($k_{a_2^m}$) of BCG dye in CTAB micellar solution using eqn. 10, the concentrations of various species involved in the equilibrium reactions *e.g.* $[D_m^{2-}]$, $[DH_m^-]$, $[D_w^{2-}]$ and $[DH_w^-]$ are required to be determined first. For that, the stepwise dissociation equilibriums were considered in the following way. In view of the equilibrium-I in aqueous phase (**Scheme-I**), we can write:

$$k_{a_2^w} = \frac{[D_w^{2-}][H_w^+]}{[DH_w^-]} \quad (11)$$

$$\text{or} \quad [D_w^{2-}] - \left(\frac{k_{a_2^w}}{[H_w^+]}\right)[DH_w^-] = 0 \quad (12)$$

In absence of the surfactant, the total concentration of dye ($[D_0]$) can be expressed as:

$$[D_0] - [DH_w^-] - [D_w^{2-}] = 0 \quad (13)$$

Therefore, eqns. 12 and 13 can be solved simultaneously to get the values of $[DH_w^-]$ and $[D_w^{2-}]$.

At the outset, hypothesizing the interaction solely between the dianionic form of BCG (D_w^{2-}) and the CTAB-micelle, one can anticipate an equilibrium of the following nature:

$$[D_w^{2-}] + [DH_w^-] + [S_m] \underset{}{\overset{k_{ass}}{\rightleftharpoons}} [D_m^{2-}] \quad (14)$$

where $[S_m]$ is the total concentration of micellized surfactant (*i.e.* total concentration of CTAB $[S_0]$ – CMC of CTAB) and k_{ass} is the association constant or the binding constant of BCG with CTAB. Therefore, we get:

$$k_{ass} = \frac{[D_m^{2-}]}{[DH_w^-][D_w^{2-}][S_m]} \quad (15)$$

$$\text{or} \quad [D_m^{2-}] - \frac{k_{ass}[S_m]}{[DH_w^-][D_w^{2-}]} = 0 \quad (16)$$

Now, total concentration of dye under the present condition can be written as:

$$[D_0] - [DH_w^-] - [D_w^{2-}] - [D_m^{2-}] = 0 \quad (17)$$

Consequently, solving eqns. 16 and 17 simultaneously will yield the concentrations of $[D_m^{2-}]$, along with refined values for concentrations of $[DH_w^{2-}]$ and $[D_w^{2-}]$.

In the next step solubilization of both the monoanionic and the dianionic form of BCG in CTAB micelle is considered. Under this circumstance, the total dye concentration ($[D_0]$) is expressed by the following equation:

$$[D_0] = [DH_w^-] + [D_w^{2-}] + [DH_m^-] + [D_m^{2-}] \quad (18)$$

$$\text{or} \quad [DH_m^-] = [D_0] - ([DH_w^-] + [D_w^{2-}] + [D_m^{2-}] = 0 \quad (19)$$

Once more, considering the equilibrium-III between the dianionic and monoanionic forms of BCG (**Scheme-I**) that are solubilized in the CTAB-micelle, we can express:

$$k_{a_2^m} = \frac{[D_m^{2-}][H_m^+]}{[DH_m^-]} \quad (20)$$

$$\text{or,} \quad [DH_m^-] - \left(\frac{[H_m^+]}{k_{a_2^m}}\right)[D_m^{2-}] = 0 \quad (21)$$

Assuming that the indicator dissociation constant is an intrinsic property of the dye and remains consistent in both the micellar pseudo phase and the water phase ($pK_{a_2^m} = pK_{a_2^w}$), eqn. 21 can be expressed as:

$$[DH_m^-] - \left(\frac{[H_m^+]}{k_{a_2^w}}\right)[D_m^{2-}] = 0 \quad (22)$$

Furthermore, if the apparent change in the $pK_{a_2^m}$ is attributed to the variance in pH of the micellar medium, eqn. 20 can be expressed as:

$$[DH_m^-] - \left(\frac{[H_w^+]}{k_{a_2^m}}\right)[D_m^{2-}] = 0 \quad (23)$$

By comparing eqns. 22 and 23, eqn. 24 can be written as:

$$[H_m^+] = \left(\frac{k_{a_2^w}[H_w^+]}{[k_{a_2^m}]} \right) \quad (24)$$

An iterative method using MS excel solver with GRG non-linear regression analysis was employed to solve the system of equations (eqns. 12, 13, 16, 17, 19, 21 and 24) simultaneously. This method adjusts the values of $[D_m^{2-}]$, $[DH_m^-]$,$[D_w^{2-}]$, $[DH_w^-]$ and $[H_m^+]$ iteratively until a set of values are found that satisfy all equations and all the equilibrium constraints within specified tolerances. The obtained concentrations were then substituted into eqn. 10, allowing for the calculation of apparent dissociation constant ($k_{a_2^m}$) of BCG in the micellar medium (Table-4). The determined $k_{a_2^m}$ value provides insight into the dissociation behaviour of BCG in the CTAB micellar solution, enabling comparisons with theoretical predictions and experimental data.

The plots in Fig. 5 illustrate the theoretical $pk_{a_2^m}$ values calculated using method-2, where the concentrations of CTAB (post-CMC) were varied at the fixed aqueous pH values of 3.8, 5.3 and 7.0 each. It was found that at pH 3.8 the $pk_{a_2^m}$ decreases as the concentration of CTAB increases in the post-CMC region. At pH 5.3 and pH 7.0, the $pk_{a_2^m}$ initially increases with increasing surfactant concentration and then stabilizes, becoming almost constant. The average $pk_{a_2^m}$ values obtained using method-2 for each pH medium are presented in Table-5. These values are compared with the calculated $pk_{a_2^m}$ values using method-1. The observed trends in $pk_{a_2^m}$ with varying CTAB concentrations and pH levels indicates surfactant concentration and pH have an influence on the dissociation behaviour of BCG in the micellar medium.

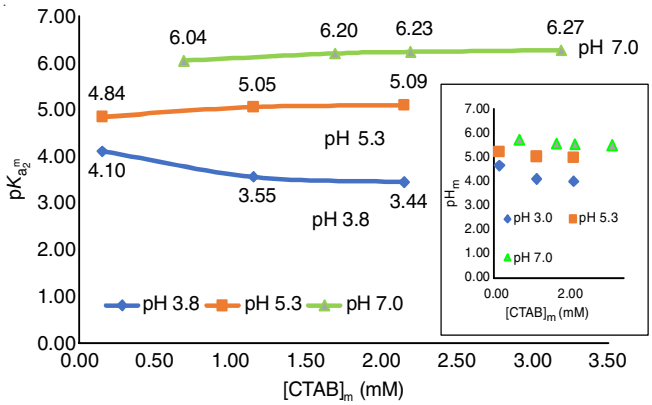

Fig. 5. Plot of $pK_{a_2^m}$ with the variation in $[CTAB]_m$ in mM in the fixed aqueous pH of 3.8, 5.3, and 7.0 respectively at 303 K determined by Method-2. [Inset: variation in micellar pH_m *vs.* $[CTAB]_m$ in mM at the fixed aqueous pH of 3.8, 5.3 and 7.0 respectively at 303 K]

The $pK_{a_2^m}$ values of BCG were additionally determined using absorbance data obtained from experimental measurements (Table-5). This calculation was performed using the following equation:

$$pk_a = pH - \log\left(\frac{(A_b - A_x)}{(A_x - A_a)} \right) \quad (25)$$

where A_a is the absorbance of BCG in strong acidic medium monitoring $\lambda_{max} = 616$ nm corresponding to the dianionic form of BCG. Similarly, A_b and A_x are the absorbance of 616 nm peak of BCG in strong basic medium and at an intermediate pH in micellar solution. The calculated values of $pk_{a_2^m}$ obtained by experimental method and theoretical method-2 were found to be nearly equivalent.

TABLE-4
CALCULATED $[D_m^{2-}]$, $[DH_m^-]$,$[D_2^{2-}]$, $[DH_w^-]$ AND $[H_m^+]$ BY ITERATIVE METHOD USING MS EXCEL SOLVER WITH GRG NON-LINEAR REGRESSION ANALYSIS

	K_{ass}	$[H_w^+]$	$[S_m]$	$[D_w^{2-}]$	$[DH_w^-]$	$[DH_m^-]$	$[D_m^{2-}]$	$pk_{a_2^m}$	pH_m
pH 3.8	2.08×10^3	1.58×10^{-4}	1.50×10^{-4}	8.30×10^{-6}	6.00×10^{-5}	6.93×10^{-6}	2.49×10^{-5}	4.10	4.7
			1.15×10^{-3}	2.60×10^{-6}	1.90×10^{-5}	1.70×10^{-5}	6.12×10^{-5}	3.55	4.1
			2.15×10^{-3}	1.60×10^{-6}	1.10×10^{-5}	1.89×10^{-5}	6.81×10^{-5}	3.44	4.0
pH 5.3	1.41×10^3	5.0×10^{-6}	1.50×10^{-4}	5.84×10^{-5}	1.47×10^{-5}	1.12×10^{-5}	1.57×10^{-5}	4.84	5.2
			1.15×10^{-3}	2.09×10^{-5}	5.26×10^{-6}	3.08×10^{-5}	4.31×10^{-5}	5.05	5.0
			2.15×10^{-3}	1.28×10^{-5}	3.20×10^{-6}	3.50×10^{-5}	4.90×10^{-5}	5.09	5.0
pH 7.0	1.25×10^3	1.00×10^{-7}	6.90×10^{-4}	4.83×10^{-5}	2.21×10^{-7}	9.72×10^{-5}	4.18×10^{-5}	6.04	5.7
			1.69×10^{-3}	2.76×10^{-5}	1.26×10^{-7}	1.36×10^{-5}	5.86×10^{-5}	6.20	5.6
			2.19×10^{-3}	2.28×10^{-5}	1.04×10^{-7}	1.46×10^{-5}	6.26×10^{-5}	6.23	5.5
			3.19×10^{-3}	1.68×10^{-5}	9.90×10^{-8}	1.57×10^{-5}	6.74×10^{-5}	6.27	5.5
$k_{a_2^w}$	1.70×10^{-5}		$[D_o]$	1.00×10^{-4}					

TABLE-5
INDICATOR DISSOCIATION CONSTANTS ($pk_{a_2^m}$) OF BCG IN CTAB MICELLAR MEDIA AND MICELLAR pH_m AT 303 K DETERMINED BY METHOD-1 AND METHOD-2

pH	Experimental		Theoretical		
	$pk_{a_2^w}$	$pk_{a_2^m}$	$pk_{a_2^m}$		Micellar surface pH_m
			Method 1	Method 2*	Method 2*
3.8		3.74	3.83	3.70	4.3
5.3	4.87	4.61	4.25	4.99	5.1
7.0		6.42	5.02	6.19	5.6

*Average values of Table-4.

The equilibrium-III in the micellar medium, as depicted in **Scheme-I**, suggests that as the $pk_{a_2^m}$ values decrease, there should be a corresponding decrease in the micellar pH_m values (resulting in an increase in the concentration of $[H_m^+]$) and *vice-versa*. This trend was observed in the BCG-CTAB system when the experiment was conducted at a fixed pH medium of 3.8. However, when the pH of the medium was altered to pH 5.3 or pH 7.0, an interesting observation was made: with an increase in $pk_{a_2^m}$ values, there was a slight increase in the magnitude of $[H_m^+]$ ions (resulting in a decrease in pH_m) as depicted in Fig. 5 (inset). This phenomenon does not follow the expected trend observed at pH 3.8. A probable explanation for this unexpected behaviour could be attributed to the preferential solvation of basic form of BCG (D_w^{2-}) over the acidic form (DH_w^-) within the micellar medium. This preferential solvation might lead to an increase in the concentration of $[D_m^{2-}]$ and $[H_m^+]$ *via* equilibrium-IV as outlined in **Scheme-I**.

Therefore, the alterations in the ratio of the intensity of absorption of band-3/band-2 of BCG in CTAB micelles were observed to be correlated to a delicate balance between the changes in the magnitude of the indicator dissociation constant ($pk_{a_2^m}$) of BCG (equilibrium-III, **Scheme-I**) and the preferential solvation of the basic form of BCG (D_m^{2-}) within the micellar medium (equilibrium-IV, **Scheme-I**). This intricate interplay highlights the complexity of the BCG-CTAB system and underscores the importance of considering multiple equilibrium processes when interpreting the experimental results.

Conclusion

This work analyzes the dissociation equilibrium of bromocresol green (BCG) dye in cetyltrimethylammonium bromide (CTAB) micellar media using spectrophotometric techniques. As CTAB concentration increased in the pre-micellar region, the band-3/band-2 intensity ratio in BCG absorption spectra increases, indicating more BCG molecules preferentially interacting with CTAB micelles. The saturation in the absorption ratio at the CMC signifies complete BCG solubilization in micelles, where all micelles are fully loaded with BCG, halting further ratio increase. In post-micellar region, as CTAB concentration increases, the BCG absorption ratio (band-3/band-2) slightly decreases, indicating potential changes in BCG's dissociation equilibrium and its interaction with CTAB micelles. The magnitudes of the partition coefficient and the binding constants were observed to decrease with the increase in the pH of medium. The influence of CTAB micellar media on the dissociation equilibria of BCG was examined by comparing experimentally determined $pK_{a_2^m}$ values with those obtained through theoretical methods. The pH of the aqueous and micellar media significantly affects $pK_{a_2^m}$ values. In pH 3.8, $pK_{a_2^m}$ decreases with increasing micellized CTAB concentration, while in pH 5.3 and pH 7.0, it increases. This variation is attributed to changes in the solubilization of BCG's dianionic form in the CTAB micellar medium, which depends on aqueous pH. The observed absorption band intensities in the micellar medium correlate with these $pK_{a_2^m}$ differences. Overall, the study provides insights into the complex interplay between solubilization behaviour, dissociation equilibria and the presence of CTAB micellar media, which can have implications for various applications involving BCG dye.

CONFLICT OF INTEREST

The authors declare that there is no conflict of interests regarding the publication of this article.

REFERENCES

1. S.A. Shapovalov, *Colorants*, **1**, 5 (2021); https://doi.org/10.3390/colorants1010003
2. L.R. Magnaghi, C. Zanoni, G. Alberti and R. Biesuz, *Anal. Chim. Acta*, **1281**, 341807 (2023); https://doi.org/10.1016/j.aca.2023.341807
3. E. Barni, P. Savarino and G. Viscardi, *Acc. Chem. Res.*, **24**, 98 (1991); https://doi.org/10.1021/ar00004a002
4. A. Eldidamony, S. Hafeez and A. Saad, *J. Appl. Pharm. Sci.*, **5**, 122 (2015); https://doi.org/10.7324/JAPS.2015.50719
5. R.K. Dutta and S.N. Bhat, *Can. J. Chem.*, **71**, 1785 (1993); https://doi.org/10.1139/v93-221
6. R.K. Dutta, R. Chowdhury and S.N. Bhat, *J. Chem. Soc., Faraday Trans.*, **91**, 681 (1995); https://doi.org/10.1039/FT9959100681
7. N.O. Mchedlov-Petrossyan, V.S. Farafonov and A.V. Lebed, *J. Mol. Liq.*, **264**, 683 (2018); https://doi.org/10.1016/j.molliq.2018.05.076
8. P.M. Saikia, A. Kalita, B. Gohain, S. Sarma and R.K. Dutta, *Colloids Surf. A Physicochem. Eng. Asp.*, **216**, 21 (2003); https://doi.org/10.1016/S0927-7757(02)00545-9
9. F. Ahmadi, M.A. Daneshmehr and M. Rahimi, *Spectrochim. Acta A Mol. Biomol. Spectrosc.*, **67**, 412 (2007); https://doi.org/10.1016/j.saa.2006.07.033
10. N.O. Mchedlov-Petrossyan, V.S. Farafonov, T.A. Cheipesh, D.A. Nerukh, S.V. Shekhovtsov and A.V. Lebed, *Colloids Surf. A Physicochem. Eng. Asp.*, **565**, 97 (2019); https://doi.org/10.1016/j.colsurfa.2018.12.048
11. P.M. Saikia, M. Bora and R.K. Dutta, *J. Colloid Interface Sci.*, **285**, 382 (2005); https://doi.org/10.1016/j.jcis.2004.11.047
12. A. Pastore, D. Badocco, S. Bogialli, L. Cappellin and P. Pastore, *Microchem. J.*, **160**, 105605 (2021); https://doi.org/10.1016/j.microc.2020.105605
13. M. Islam, M. Hossain, S. Mahbub, M.A. Hoque, D. Kumar, S.M. Wabaidur, M.A. Habila, M.M. Al-Anazy and M. Kabir, *Mol. Phys.*, **119**, e1925364 (2021); https://doi.org/10.1080/00268976.2021.1925364
14. S.M. Islam, S. Mahbub, M.A. Ahmad, S.K. Mustafa, F.A. Alasmary and M.A. Hoque, *Mol. Phys.*, **119**, e1945157 (2021); https://doi.org/10.1080/00268976.2021.1945157
15. S. Fassi, I. Bousnoubra, T. Sehili and K. Djebbar, *J. Mater. Environ. Sci.*, **3**, 732 (2012).
16. A. Shokrollahi and F. Firoozbakht, *Beni Suef Univ. J. Basic Appl. Sci.*, **5**, 13 (2016); https://doi.org/10.1016/j.bjbas.2016.02.003
17. M. Bielska, A. Sobczyn'ska and K. Prochaska, *Dyes Pigments*, **80**, 201 (2009); https://doi.org/10.1016/j.dyepig.2008.05.009
18. S. Gokturk, *J. Photochem. Photobiol. Chem.*, **169**, 115 (2005); https://doi.org/10.1016/j.jphotochem.2004.06.009
19. M.E.D. Garcia and A. Sanz-Medel, *Talanta*, **33**, 255 (1986); https://doi.org/10.1016/0039-9140(86)80060-1
20. B. Simonèiè and J. Špan, *Dyes Pigments*, **36**, 1 (1998); https://doi.org/10.1016/S0143-7208(97)00001-6
21. C.K. Yadav, A. Bhattarai, T.P. Niraula, A.P. Yadav, M.K. Adhikari, Y.P. Yadav, D. Yadav and S. Singh, *Amrit J.*, **3**, 66 (2023); https://doi.org/10.3126/amritj.v3i1.61543
22. O. Èudina, K. Karljikovic-Rajic, I. Ruvarac-Bugarèic and I. Jankovic, *Colloids Surf. A Physicochem. Eng. Asp.*, **256**, 225 (2005); https://doi.org/10.1016/j.colsurfa.2005.01.023

23. S.M.Z. Andrabi, M.A. Malik and Z. Khan, *Colloids Surf. A Physicochem. Eng. Asp.*, **299**, 58 (2007); https://doi.org/10.1016/j.colsurfa.2006.11.018
24. S.S. Shah, K. Naeem, S.W.H. Shah and G.M. Laghari, *Colloids Surf. A Physicochem. Eng. Asp.*, **168**, 77 (2000); https://doi.org/10.1016/S0927-7757(99)00520-8
25. S.S. Shah, M.S. Khan, H. Ullah and M.A. Awan, *J. Colloid Interface Sci.*, **186**, 382 (1997); https://doi.org/10.1006/jcis.1996.4649
26. M.A. Awan and S.S. Shah, *Colloids Surf. A Physicochem. Eng. Asp.*, **122**, 97 (1997); https://doi.org/10.1016/S0927-7757(96)03825-3
27. S. Gokturk and M. Tuncay, *Spectrochim. Acta A Mol. Biomol. Spectrosc.*, **59**, 1857 (2003); https://doi.org/10.1016/S1386-1425(02)00418-3
28. N. Shahi, S. K. Shah, A. P. Yadav, A. Bhattarai, *GU J. Sci.,* **36**, 120 (2023); https://doi.org/10.35378/gujs.978088
29. M.S. Ramadan, N.M. El-Mallah, G.M. Nabil and S.M. Abd-Elmenem, *J. Dispers. Sci. Technol.*, **40**, 1110 (2019); https://doi.org/10.1080/01932691.2018.1496837
30. Z.A. Khan and A.S. Al-Bogami, *Asian J. Chem.*, **25**, 10499 (2013); https://doi.org/10.14233/ajchem.2013.15768
31. S. Noor, M.B. Taj and A. Ashar, *J. Mol. Liq.*, **330**, 115613 (2021); https://doi.org/10.1016/j.molliq.2021.115613
32. M. Sarkar and S. Poddar, *Spectrochim. Acta A Mol. Biomol. Spectrosc.*, **55**, 1737 (1999); https://doi.org/10.1016/S1386-1425(98)00344-8
33. P. Shah, S.K. Jha and A. Bhattarai, *J. Mol. Liq.*, **340**, 117200 (2021); https://doi.org/10.1016/j.molliq.2021.117200
34. M. Irfan, M. Usman, A. Mansha, N. Rasool, M. Ibrahim, U.A. Rana, M. Siddiq, M. Zia-Ul-Haq, H.Z.E. Jaafar and S.U.-D. Khan, *Sci. World J.*, **2014**, 540975 (2014); https://doi.org/10.1155/2014/540975
35. P. Shah, N. Jha and A. Bhattarai, *J. Chem.*, **2020**, 5292385 (2020); https://doi.org/10.1155/2020/5292385
36. D.S. Pellosi, B.M. Estevão, J. Semensato, D. Severino, M.S. Baptista, M.J. Politi, N. Hioka and W. Caetano, *J. Photochem. Photobiol. Chem.*, **247**, 8 (2012); https://doi.org/10.1016/j.jphotochem.2012.07.009
37. H. Kawamura, M. Manabe, Y. Miyamoto, Y. Fujita and S. Tokunaga, *J. Phys. Chem.*, **93**, 5536 (1989); https://doi.org/10.1021/j100351a042
38. H.A. Benesi and J.H. Hildebrand, *J. Am. Chem. Soc.*, **71**, 2703 (1949); https://doi.org/10.1021/ja01176a030
39. B. Boruah, B. Gohain, P.M. Saikia, M. Borah and R.K. Dutta, *J. Mol. Liq.*, **160**, 50 (2011); https://doi.org/10.1016/j.molliq.2011.02.014
40. R. Sabaté, M. Gallardo, A. de la Maza and J. Estelrich, *Langmuir*, **17**, 6433 (2001); https://doi.org/10.1021/la010463y